Modelling interaction forces at a curved physical human-exoskeleton interface

DHM2020
L. Hanson et al. (Eds.)

doi:10.3233/ATDE200028

Modelling Interaction Forces at a Curved Physical Human-Exoskeleton Interface

Divyaksh Subhash CHANDER [1] and Maria Pia CAVATORTA
Department of Mechanical and Aerospace Engineering, Politecnico di Torino, Corso Duca degli Abruzzi, 24, 10129 Torino, Italy

Abstract. In virtual modelling of exoskeletons, the human-exoskeleton interface is often simplified by modelling the interface forces at a single point instead of contact forces due to the straps or cuffs. In the past, force-generating elements (FGEs) have been used to predict ground reaction forces. However, unlike the ground, which is a planar surface, the human-exoskeleton interface presents curved surfaces. This work discusses the modifications required for using the FGEs for predicting the curved human-exoskeleton interface forces of a passive lower-limb exoskeleton, the Chairless Chair. A pressure mat was positioned at the human-exoskeleton interface to measure the area of contact and the centre of pressure (CoP) in three different sitting conditions. The strength of the FGEs was analysed in detail and its optimization based on the model outputs is discussed. The strength affects the model assistance and the CoP, and these outputs could be used to identify the optimal value of the strength. The strength of the FGEs affects the biomechanical outputs from the model also. Therefore, it is crucial to select the correct value of the strength. The results of this work would be useful for the detailed modelling of the human-exoskeleton interface.

Keywords. Human-Exoskeleton Interaction, Interface Forces, Curved Surface, Passive Exoskeleton, Musculoskeletal Model

1. Introduction

Virtual assessment of exoskeletons is often used during the design and redesign phase to optimize the exoskeleton. The level of assistance or the design of the exoskeleton could be optimized considering the end-user or the activity [1–3]. As the end-user of an exoskeleton is a human, biomechanical analysis plays a key role in assessing the exoskeleton. Virtual assessment of the exoskeleton through multibody dynamics is often used in the literature for biomechanical analysis. Such an assessment requires a model of the human, a model of the exoskeleton and an interaction model to connect the human and the exoskeleton models. Subsequently, a comparison is made between the with and without exoskeleton cases for the target activity.

Often in multibody dynamics, the interaction between the human and the exoskeleton is modelled through kinematic joints [1, 4, 5]. Rigid kinematic joints are used to fix the different attachment points of the exoskeleton to the corresponding points on the human model. Such joints constrain all the translational and rotational degrees of freedom and provide reaction forces and moments in these constraints. Another approach to model the interface forces between the human and the exoskeleton

[1] Corresponding Author, Email: chander.divyaksh@polito.it.

is to use force-generating elements (FGEs) to create reaction forces in the necessary constraints in the model [6]. However, both the approaches are not a realistic representation of the actual interface between the human and the exoskeleton. The human-exoskeleton interface usually consists of straps or moulded surfaces to fix the exoskeleton to the user and to provide support and assistance. The presence of straps or moulded surface leads to the generation of frictional forces. The straps must be closed tightly for generating enough frictional and normal forces to rigidly attach the exoskeleton to the user. Frictional forces are not accounted for by the kinematic joints or the FGEs (unless the FGEs are configured to). Not modelling friction at the interface could result in an unrealistic interaction force at the human-exoskeleton interface.

The FGEs could be configured to simulate contact forces, including frictional forces. Such an approach has been used extensively to predict ground reaction forces (GRFs) [7, 8]. Recently, this approach has also been used to predict reaction forces at the human-exoskeleton interface. The effect of the interface model on the biomechanical outputs was studied in [9] and it was observed that using the GRF prediction method at the human-exoskeleton interface resulted in a more reasonable trend of the knee moment compared to using a rigid kinematic joint at the interface. However, a limitation of the GRF prediction method, as far as the human-exoskeleton interface is concerned, is that the method is suitable for predicting contact forces at planar surfaces only, such as the ground. In the case of exoskeletons, the straps wrap around the body or the moulded surfaces are shaped according to the shape of the matching body part. Thus, the approach must be modified to predict contact forces at the human-exoskeleton interface.

The aim of this work is to modify the approach of the GRF prediction method to predict the contact forces at a curved human-exoskeleton interface. In this work, the modifications required to the existing method for planar surfaces will be discussed and indications would be provided for selecting the parameters of the modified method suitable for curved surfaces.

2. Method

This work builds on the existing work [9] that used the GRF prediction method to estimate the interface forces at the human-exoskeleton interface of a passive exoskeleton for the lower limbs, the Chairless Chair® (noonee AG, Switzerland). The exchange of forces was considered in a limited area of contact on the seat that was assumed planar in [9]. The curved surface of the seat prevented the use of the entire seated area for the exchange of forces by the GRF prediction method as the method is intended for planar surfaces, such as the ground. The current work aims to modify the approach of the GRF prediction method to estimate interface forces at curved surfaces so that the entire seated area of the Chairless Chair could be used for the exchange of forces at the human-exoskeleton interface.

The Chairless Chair consists of two mechanical legs that are loosely attached behind the user's legs. The exoskeleton allows the user to walk and as the user starts to sit, the exoskeleton legs touch the ground and bend at their central revolute joint. The exoskeleton legs block at a user-selected position and provide static support to the user in the seated posture, like a regular chair. The sitting height of the exoskeleton can be continuously adjusted between a minimum height, defined as the low-seat configuration, and a maximum height, defined as the high-seat configuration.

2.1. Experimental pressure maps

The human-exoskeleton interface was studied in three different sitting conditions: the low-seat, the high-seat, and the comfort-seat configuration, which is defined as the seat height selected by the user as the most comfortable. The different seat heights provided different seat inclinations and contact conditions, resulting in a changed seated posture and the support available from the exoskeleton. Previous studies have reported that the high seat configuration led to an increased tendency of slip [10, 11]. A pressure mat (PX200:20.40.05, XSensor) was placed on the exoskeleton seat for the right leg and recorded the human-exoskeleton interface pressure at 60 Hz. The pressure mat served to determine the area of contact at the interface and to compare the empirical and the virtual centre of pressure (CoP). The data of the pressure mat was mirrored about the sagittal plane for the left leg due to the symmetry of the posture. The pressure mat had a total of 800 cells arranged in an array of 40 x 20, with each cell having an area of 0.51 x 0.51 cm^2. The body weight distribution between the human and the exoskeleton was measured using a scale. A static resting posture was used across the conditions to avoid unnecessary variables in this study. The trials were done by a male subject (163.0 cm and 73.8 kg) who was trained in the use of the exoskeleton. As described in a prior study, the percentage of body weight supported by the exoskeleton was consistent among different users provided that they were trained in the use of the Chairless Chair [11]. The Chairless Chair was adjusted to the anthropometry of the user by setting both the lower and the upper half of the exoskeleton leg to their smallest lengths in these trials. After the subject assumed the seated posture and provided a verbal confirmation of feeling stable, data were recorded for at least three seconds in the static resting posture (Figure 1). For each test condition, three trials were done, and the data were averaged over the three trials.

2.2. Musculoskeletal modelling

A commercially available software, AnyBody Modelling Systems (AMS) (version 7.1.2, AnyBody Technology A/S, Denmark) was used to develop the model for the biomechanical analysis using the musculoskeletal human model available in the AnyBody Managed Model Repository version 2.1.1 [12]. The human model was scaled to the subject height and weight using length-mass-fat scaling law. AMS models human muscles as unidirectional FGEs and uses a multibody dynamics approach to analyse the musculoskeletal system. It uses inverse dynamics analysis to estimate the internal muscle and joint reaction forces given the external forces and motion data. As the body contains an excess of muscles than necessary to solve the dynamic equilibrium, the inverse dynamics analysis equations are framed as an optimisation problem to determine the muscle recruitment. In this work, the polynomial criterion with power 3 was used for the muscle recruitment problem [13].

A computer-aided design (CAD) model of the exoskeleton was created using SolidWorks® 2017 (Dassault Systèmes SOLIDWORKS Corporation) and translated into an AMS compatible script file using the AnyExp4SOLIDWORKS® plugin (version 1.1.0, AnyBody Technology A/S, Denmark). The central revolute joint between the upper and the lower half of the exoskeleton was defined to produce all the reaction forces and moments necessary to support the user in the seated posture.

A static model of the trials was developed with the human and the exoskeleton models positioned according to the experimentally observed postures and positions

(Figure 1). GRFs at the human foot and the exoskeleton base were estimated in the model as described in [9], using the method reported in [8], by creating virtual force plates (VFPs) in the model.

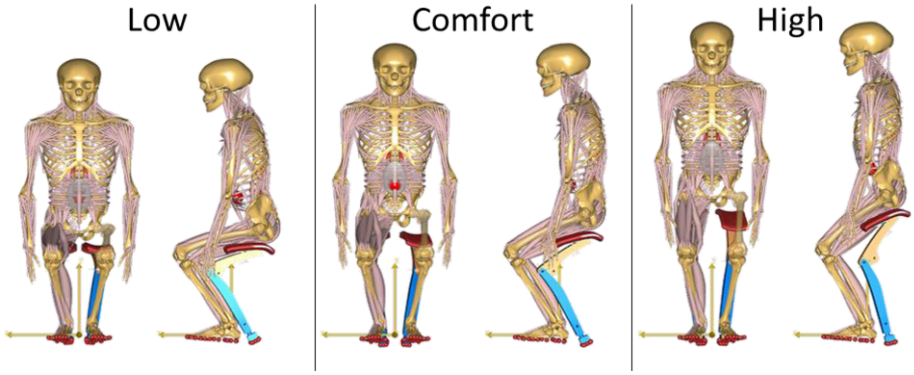

Figure 1. Virtual models of the low, comfort and high seat. Muscles of the left leg are hidden.

2.3. Human-exoskeleton interaction forces

The human-exoskeleton interaction forces were estimated by modifying the approach of GRF prediction method to predict reaction forces at the human-exoskeleton interface, which usually consists of a curved surface. Instead of using a single VFP with multiple contact nodes, multiple VFPs were distributed over the surface of the exoskeleton seat. Each VFP was positioned tangentially at its centre to the seat surface and consisted of a single contact node positioned correspondingly on the human model to ensure contact. The orientation of the VFP determined the normal and shear directions. The approach of using multiple VFPs has been used previously in [14] for predicting GRFs.

The presence of multiple VFPs allowed not just a more realistic representation of the curved surface but also allowed individual control of these VFPs. This was especially needed for the Chairless Chair, where different sitting heights resulted in different areas of contact. Thus, the empirically observed area of contact was used as an input in the model. The model also consisted of an array of 40 (rows) x 20 (columns) VFPs, each corresponding to the individual cell of the pressure mat. The VFP was inactive if the pressure mat reading of the corresponding cell was zero.

At each contact node, five artificial muscles were created and configured to produce the contact forces just as in the GRF prediction method [8]. The contact forces from the individual VFPs were processed to obtain the location of the centre of pressure (CoP) relative to the seat surface. Whereas the percentage of body weight supported by the exoskeleton was calculated as the difference between the subject weight and the weight supported by the legs of the subject.

A key parameter of these artificial contact muscles is the strength of the muscles or the maximum force that these contact muscles can produce. In [14], the maximum force was selected based on a parametric study. Similarly, a parametric study was performed in this work as well. Figure 2 shows the empirical pressure maps for the left leg and the corresponding virtual pressure maps for different values of the strength (S_0) of the artificial contact muscles. The first (top) and the last (bottom) row of the pressure maps correspond to the back and the front edges of the seat. It can be observed that high values of the strength resulted in an uneven utilization of the surface of the

seat. The solver found the exchange of the interaction forces at the rear of the exoskeleton seat to be biomechanically advantageous, such that at S_0 = 150 N, most of the seat surface was left unutilized. Consequently, the pressure in the limited area of contact far exceeded the pressure threshold of 2 N/cm^2 for discomfort [15]. On the other hand, at low values of strength, a greater surface of the exoskeleton seat was used for the interaction forces, nonetheless, with a preference for the rear portion of the exoskeleton seat for the exchange of forces.

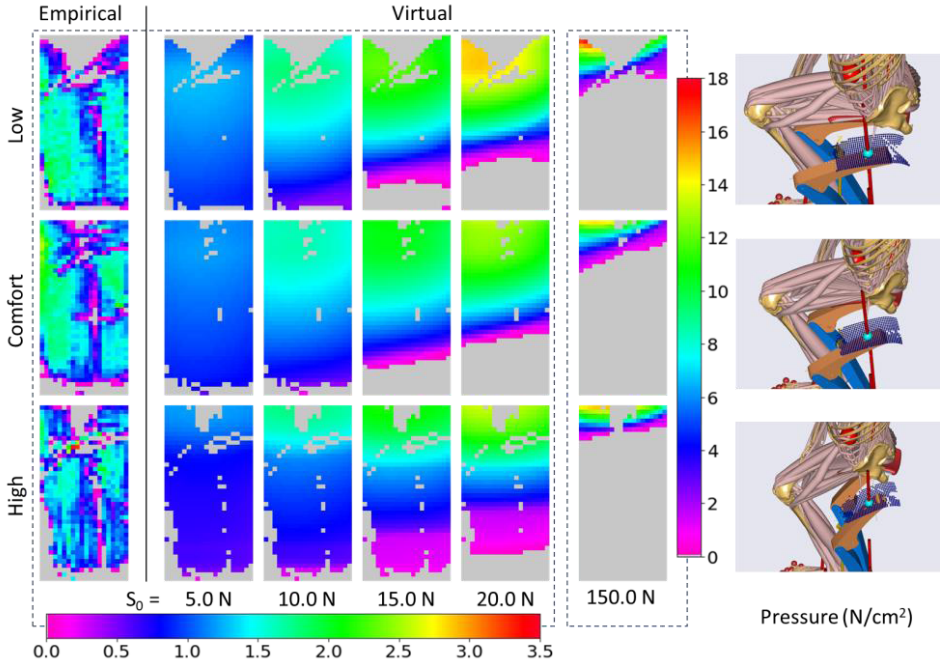

Figure 2. Empirical and virtual pressure maps for the left leg. S_0 is the strength of the contact muscles.

The preference of the solver for utilizing the rear portion of the seat to support the subject was manually offset. The strength of the artificial contact muscles at the rear of the seat was reduced relative to the front of the seat. The row of the VFP determined its position along the length of the seat. The strength of the artificial contact muscles at each VFP was given as:

$$S_{ij} = \begin{cases} 0.0 & \text{if } P_{ij} = 0.0 \\ S_0 \text{ x } [c_1 + (i\text{-}1) \text{ x } (c_2 - c_1)/39] & \text{if } P_{ij} > 0.0 \end{cases} \quad (1)$$

Where,

S_{ij} is the strength of the contact muscles at the i^{th} row and j^{th} column.

P_{ij} is the recorded pressure of the cell at the i^{th} row and j^{th} column.

S_0 is a constant factor for multiplying the strength.

c_1 and c_2 are constants for controlling the linear gradient of strength.

i is the row number.

Thus, strength at the first row (i = 1) was S_0 x c_1, while the strength at the last row (i = 40) was S_0 x c_2.

3. Results and discussion

This work aimed to model the human-exoskeleton interface forces for a curved surface, study the model parameters in detail, and identify strategies to select these parameters. This section discusses the results of the change in the strength of the contact muscles and its effect on the interaction forces and the biomechanical outputs.

3.1. Interaction forces

Figure 3 plots the percentage of body weight supported by the exoskeleton and the centre of pressure (CoP) for different values of the strength of the contact muscles, along with the empirically observed values. The position of the CoP was measured from the front edge of the seat along the length of the seat. The length of the seat is 20.5 cm. Only the front-rear location of the CoP is plotted. The location of the CoP along the seat width was not significantly affected by the strength of the artificial contact muscles and matched well with the empirically observed values. The figure shows various values of strength (defined by S_0 and indicated in the callouts in the figure) as well as the different gradients (defined by c_1 and c_2) of the strength of the contact muscles, including the constant strength without any gradient ($c_1 = c_2 = 1$).

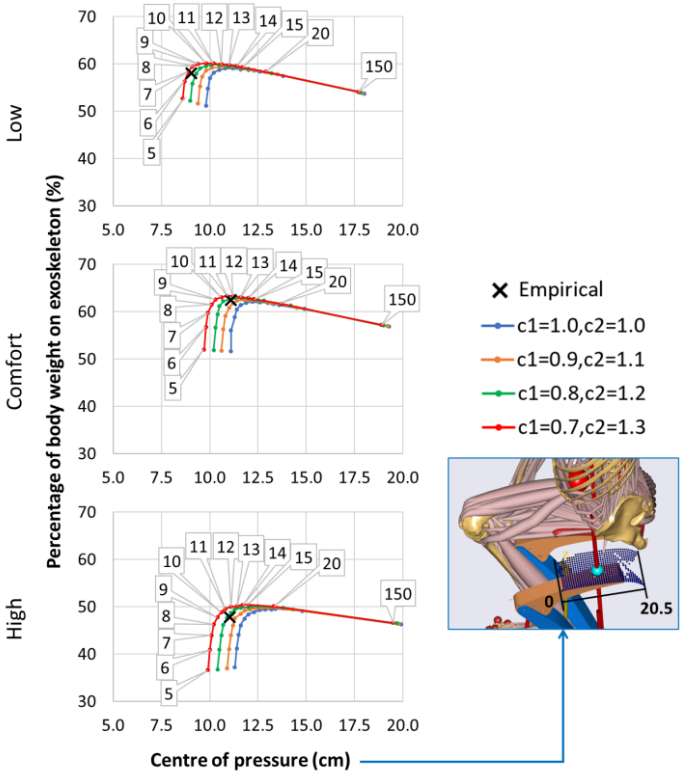

Figure 3. Exoskeleton support and the centre of pressure for different strength and gradient of the contact muscles.

An important observation is the shape of the curves in Figure 3. The curves have a similar shape for all the seat heights as well as for different gradients. It can be

observed that the exoskeleton could not provide adequate support to the user at low values of the strength of the contact muscles. Increasing the strength resulted in a uniform increase of support throughout the seat surface such that the CoP did not change until the vertex of the curve was reached. Once the vertex was reached, increasing the strength further did not increase the support provided by the exoskeleton. Instead, it resulted in a rearward shift of the CoP. The rearward shifting of the CoP could be linked to the observation made in Section 2.3 that the front part of the seat remained unutilized if the strength was large enough to allow it. Thus, the shape of the curves of Figure 3 indicates that an optimum value of strength exists around the vertex of the curve. This optimal zone of the strength should allow the required exchange of interface forces at a reasonable CoP. Figure 3 also shows that the gradient in strength resulted in an offset in the CoP location towards the front part of the seat. Higher the gradient, greater the offset. The gradient increased the strength of the contact muscles in the front of the seat relative to the rear part, resulting in a forward shift of the CoP.

The observations of Figure 3 could be compared with the approach used in [14] for selecting the maximum force of the FGEs. The authors of [14] performed a parametric study and selected the lowest value of the maximum force of the FGEs at which the GRF converged for the rest of their analyses. Similar to the observations of Figure 3, the GRF was inadequate at low values of the maximum force of the FGEs, while increasing the maximum force beyond the threshold for adequate GRF did not increase the GRF further.

3.2. Biomechanical outputs

The human-exoskeleton interface is a crucial component in the analysis of the exoskeletons. The interface forces determine the assistance received by the user and can affect the biomechanical analysis. Figure 4 plots the moments at the knee and the ankle, and the activation of the vastus lateralis and gastrocnemius muscles for different strengths of the contact muscles. The figure shows that the biomechanical outputs depend on the strength of the artificial contact muscles. At values of strength lower than the optimal zone, inadequate support was available from the exoskeleton (Figure 3), and thus a greater knee extension moment was required from the user. On the other hand, high values of the strength led to an underestimation of the knee moment. At values of the strength greater than the optimal zone, the support received by the user reduced slightly, however, the CoP shifted rearwards unrealistically, resulting in a higher overall external extension moment at the knee, and thereby reducing the demand from the user. Similarly, effects on the ankle plantarflexion moment can be observed. The changes in the joint moments were also supported by the changes in the muscular effort. The activation of vastus lateralis, a knee extensor was reduced as the knee moment requirement reduced due to the increased strength of the contact muscles. Whereas the activation of the gastrocnemius increased as the plantarflexion moment at the ankle increased due to the increase in the strength of the artificial contact muscles.

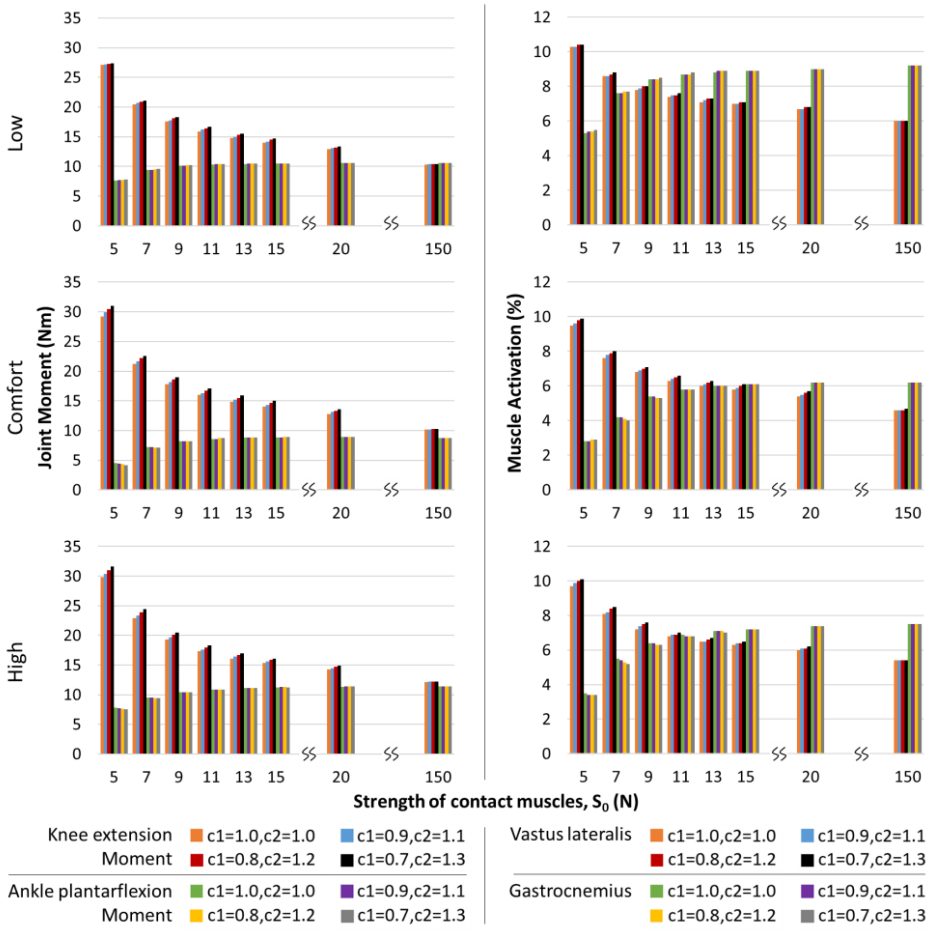

Figure 4. Joint moment and muscle activation for different strength and gradient of the contact muscles.

Figure 4 also shows a marginal effect of the strength gradient on the biomechanical outputs. For the same value of the strength (S_0) of the contact muscles, a slight variation in the biomechanical outputs was seen due to the gradient in the strength. The CoP for the gradient $c_1 = 0.8$, $c_2 = 1.2$ resulted closest to the empirically observed CoP (Figure 3). The difference in the CoP due to the strength gradient was less than 1.0 cm in the zone of optimal strength value compared to the CoP for no strength gradient. 1.0 cm is 2.7% of 37.1 cm, which is the length of the thigh of the mannequin. It is likely that this small offset in the CoP due to the strength gradient causes a small and less significant effect on the biomechanical outputs than that due to the absolute value of the strength of the contact muscles.

The model is unable to account for the deformation of the soft tissue or the seat compression and is unable to provide a realistic distribution of pressure. However, the amount of external force and its point of application are significant details in multibody analysis and can influence the biomechanical outputs as seen in this work. Thus, it is critical to pay attention to the strength of the artificial muscles introduced in this approach of distributed VFPs to simulate the human-exoskeleton interface forces.

3.3. Application to other exoskeletons

This work presented a modified approach of the GRF prediction method to estimate the human-exoskeleton interface forces at a curved surface. This approach was applied to the Chairless Chair at three different seat heights that resulted in different inclinations of the seat, different contact conditions, and different support received by the user. In this section, some considerations are discussed for applying this modelling approach to other exoskeletons.

Empirical data from the pressure mat were used as an input in the model. The contact area was used to determine the VFPs that had to be deactivated. However, this problem of determining the area of contact is also specific to the Chairless Chair as the seat is loosely attached to the user to allow different sitting heights. The area of contact, especially in the upper portion of the seat, changes with the sitting height (Figure 2). In the case of other exoskeletons, often, the human-exoskeleton interface is firmly secured using straps. In such a case it could be reasonable to assume that the entire surface area of the human-exoskeleton interface is in contact. Secondly, this work used the pressure maps to justify the use of the gradient of the strength of the contact muscles and identify the optimal gradient values. However, when no experimental data is available, the results without the strength gradient could be reasonably reliable as shown in this work. Identification of the correct strength would be a more critical factor for the analysis than the finer refinement allowed by the strength gradient.

The pressure maps highlight an important aspect of the model regarding the optimal strength of the contact muscles. Besides the convergence of the interface force, the muscle activation of the contact muscles could also be relevant. The solver cannot differentiate between the physiological and contact muscles in the optimization problem to determine the muscle forces. Low strength of the contact muscles could result in highly activated contact muscles to provide the interface forces. If the activation of the contact muscles is comparable to that of the physiological muscles, the solver might recruit some under-activated physiological muscles to unload the contact muscles. On the other hand, high strength of the contact muscles, far beyond the optimal zone, can result in the solver "exploiting" the contact muscles to reduce the biomechanical load unrealistically as seen in Figure 2 and Figure 4. Thus, it is important to find a strength of the contact muscles that is neither too high nor too low, as is also mentioned in [6]. In this study, a maximum activation of 1.5% was seen for the artificial contact muscles at strength S_0 = 5.0 N, and it reduced as S_0 was increased.

There could also be other unknowns when applying this approach to another exoskeleton, such as the behaviour of the model in dynamic activities. Depending on the phase of the movement, the model might show an unrealistic preference towards either side of the interface. In such a case, it could be desirable to taper down the strength of the artificial contact muscles on both the sides of the interface. Also, additional functions of the gradient could be explored. Further, as the strength is optimized based on the assistance received by the user, if the exoskeleton offers various assistance levels, the optimal strength could be different for each assistance level. Analogously, in this study, a subject with a substantially different body weight would require a different strength value for the Chairless Chair to support about 60% of the body weight as in the low and comfort-seat heights. A similar adjustment for the GRF estimation of obese subjects was also suggested in [14].

In conclusion, this work presented an approach to model the interaction forces at the human-exoskeleton interface. The advantage of this approach over other methods is

its ability to simulate contact forces over curved surfaces, which are typical in human-exoskeleton interfaces. On the other hand, the application of this approach requires greater attention to the model parameter than for other approaches as the model parameter can significantly affect the biomechanical outputs. It is recommended to start with a coarse grid of VFPs on the interface and make a parametric study of the strength of the artificial contact muscles without any gradient and subsequently proceed towards refining and identifying an optimal value of the strength of the contact muscles.

References

[1] Agarwal P, Neptune RR, Deshpande AD. A Simulation Framework for Virtual Prototyping of Robotic Exoskeletons. J Biomech Eng, 2016, 138(6), 061004.
[2] Jensen EF, Raunsbæk J, Lund JN, Rahman T, Rasmussen J, Castro MN. Development and simulation of a passive upper extremity orthosis for amyoplasia. J Rehabil Assist Technol Eng, 2018, 5, 1–10.
[3] Zhou L, Li Y, Bai S. A human-centered design optimization approach for robotic exoskeletons through biomechanical simulation. Rob Auton Syst, 2017, 91, 337–347.
[4] Gordon DFN, Henderson G, Vijayakumar S. Effectively Quantifying the Performance of Lower-Limb Exoskeletons Over a Range of Walking Conditions. Front Robot AI, 2018, 1–16.
[5] Harant M, Sreenivasa M, Millard M, Sarabon N, Mombaur K. Parameter optimization for passive spinal exoskeletons based on experimental data and optimal control. IEEE-RAS Int Conf Humanoid Robot, 2017, 535–540.
[6] Fournier BN, Lemaire ED, Smith AJJ, Doumit M. Modeling and Simulation of a Lower Extremity Powered Exoskeleton. IEEE Trans Neural Syst Rehabil Eng IEEE, 2018, 26(8), 1596–1603.
[7] Fluit R, Andersen MS, Kolk S, Verdonschot N, Koopman HFJM. Prediction of ground reaction forces and moments during various activities of daily living. J Biomech Elsevier, 2014, 47(10), 2321–2329.
[8] Skals S, Jung MK, Damsgaard M, Andersen MS. Prediction of ground reaction forces and moments during sports-related movements. Multibody Syst Dyn Springer Science+Business Media Dordrecht, 2017, 39(3), 175–195.
[9] Chander DS, Cavatorta MP. Modelling friction at the mechanical interface between the human and the exoskeleton. Int J Hum Factors Model Simul, 2019, 7(2), 119–136.
[10] Luger T, Cobb TJ, Seibt R, Rieger MA, Steinhilber B. Subjective Evaluation of a Passive Lower-Limb Industrial Exoskeleton Used During simulated Assembly. IISE Trans Occup Ergon Hum Factors Taylor & Francis, 2019, 7(3–4), 175–184.
[11] Spada S, Ghibaudo L, Carnazzo C, Pardo M Di, Chander DS, Gastaldi L, Cavatorta MP. Physical and Virtual Assessment of a Passive Exoskeleton. In: Proceedings of the 20th Congress of the International Ergonomics Association (IEA 2018), Springer International Publishing, Cham, 2019.
[12] Lund ME, Tørholm S, Jung M. The AnyBody Managed Model Repository (AMMR) (Version 2.1.1), 2018.
[13] Damsgaard M, Rasmussen J, Christensen ST, Surma E, Zee M de. Analysis of musculoskeletal systems in the AnyBody Modeling System. Simul Model Pract Theory, 2006, 14(8), 1100–1111.
[14] Jung Y, Jung M, Lee K, Koo S. Ground reaction force estimation using an insole-type pressure mat and joint kinematics during walking. J Biomech Elsevier, 2014, 47(11), 2693–2699.
[15] Zenk R, Mergl C, Hartung J, Sabbah O, Bubb H. Objectifying the Comfort of Car Seats. SAE Technical Paper 2006[Online], SAE International, 2006.